

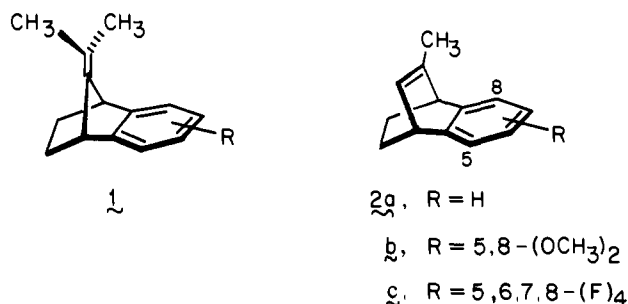
Electronic Control of Stereoselectivity. 9. The Stereochemical Course of Electrophilic Additions to Aryl-Substituted Benzobicyclo[2.2.2]octadienes¹

Leo A. Paquette,* François Bellamy,² Gregory J. Wells, Michael C. Böhm, and Rolf Gleiter*

Contribution from the Evans Chemical Laboratories, The Ohio State University, Columbus, Ohio 43210, and the Institut für Organische Chemie der Universität Heidelberg, Heidelberg, West Germany. Received February 2, 1981

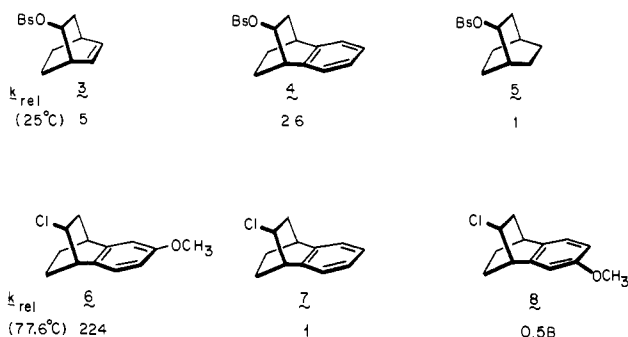
Abstract: Product and relative reactivity data have been obtained for the photooxygenation, epoxidation, cyclopropanation, oxymercuration, and hydroboration of three differently substituted (aryl) 2-methylbenzobicyclo[2.2.2]octadienes. Syn stereoselectivity was observed in every case, with the level of syn attack being highest with the tetrafluoro derivative **2c** (except in the Simmons-Smith reaction where a single isomer was produced in every case). Only small differences in rate were seen with a given reagent. Electronic interactions in these molecules were explored by photoelectron spectroscopy and MINDO/3 calculations. These combined tools served to show that through-space interaction is absent in these molecules. However, through-bond coupling in **2a** and **2b** leads to olefinic π -bond disrotation. The relative importance of this effect as well as long-range Coulomb and charge-transfer interactions is discussed. A connection between such subtle electronic influences and stereoselectivity is established, although prevailing steric effects do serve to compress somewhat the syn/anti range available to these systems.

In preceding papers,^{1,3} we explained the contrasting stereoselection exhibited by weak and strong electrophiles in their addition to the exocyclic double bond of **1** and 7-isopropylidenebornene



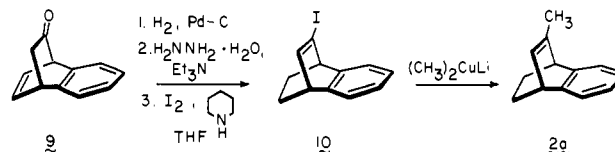
in terms of substrate response to transition state demands. When the rate-determining step is associated with a bridged ion because of the need to polarize a weak electrophilic reagent, π -bond assistance is energetically rewarding and homoaromatic involvement of the aryl ring gains considerable importance. When the electrophilicity of the reagent is high, such π -bond assistance becomes unnecessary and syn attack now prevails for complexation⁴ reasons.

In an effort to substantiate these conclusions, we have proceeded to examine the response of 2-methylbenzobicyclo[2.2.2]octadienes **2a-c** to various electrophilic reagents. This choice was predicated on the knowledge⁵ that the solvolysis rate of brosylate **4** is far less accelerated relative to **5** than is the *anti*-9-benzonorbornenyl/7-norbornenyl pair (factor of 6×10^5).⁶ When taken in tandem with the k_{rel} for **3**, this information denotes that incorporation of un-

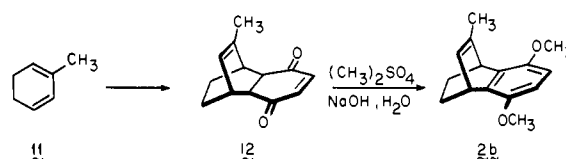


* Address correspondence as follows: L.A.P., The Ohio State University; R.G., Universität Heidelberg.

Scheme I



Scheme II



saturation clearly affects the two systems differently. There is no doubt that interaction can develop between the aromatic ring and incipient carbonium ion center in **4**. However, as attested to by the reactivity of **6** and **8** relative to that of **7**,⁷ the necessarily unsymmetrical nature of the aryl participation is restricted in degree to that maximally available to a β -arylethyl system. At issue, therefore, is the question whether this obviously reduced long-range interaction will continue to affect the outcome of electrophilic stereoselection in **2a-c** or whether more subtle electronic influences will now determine product stereochemistry (barring steric effects).

Results

Synthesis. Hydrocarbon **2a** was prepared according to Scheme I. Although ketone **9** has been described by several groups, best yields were obtained by application of Kitahonoki's procedure for the β -naphthol-maleic anhydride cycloaddition,⁸ followed by the Cimarusti-Wolinsky technique for bisdecarboxylation.⁹ Low-

(1) Part 8: Paquette, L. A.; Hertel, L. W.; Gleiter, R.; Böhm, M. C.; Beno, M. A.; Christoph, G. G., preceding paper in this issue.

(2) NATO Postdoctoral Fellow with financial support provided by the CNRS.

(3) Prior communications on this subject have also appeared: (a) Paquette, L. A.; Hertel, L. W.; Gleiter, R.; Böhm, M. J. *Am. Chem. Soc.* **1978**, *100*, 6510. (b) Hertel, L. W.; Paquette, L. A. *Ibid.* **1979**, *101*, 7620.

(4) Paquette, L. A.; Klinger, F.; Hertel, L. W. *J. Org. Chem.* **1981**, *46*, 4403.

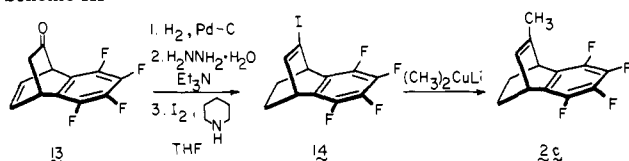
(5) Tanida, H.; Tori, K.; Kitahonoki, K. *J. Am. Chem. Soc.* **1967**, *89*, 3212.

(6) Bartlett, P. D.; Giddings, W. P. *J. Am. Chem. Soc.* **1960**, *82*, 1240.

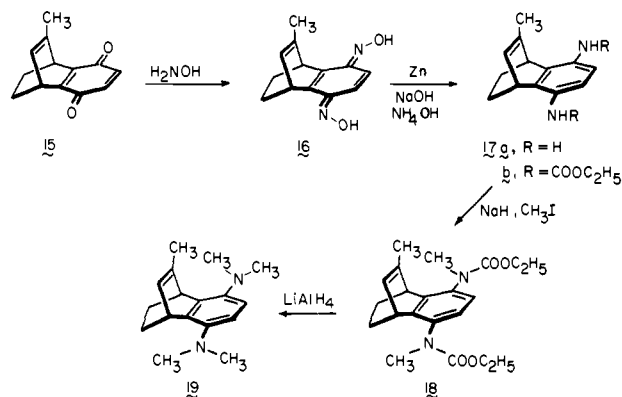
(7) Tanida, H.; Miyazaki, S. *J. Org. Chem.* **1971**, *36*, 425.

(8) Kitahonoki, K.; Takedo, K. *Yakugaku Zasshi* **1953**, *73*, 280.

Scheme III



Scheme IV



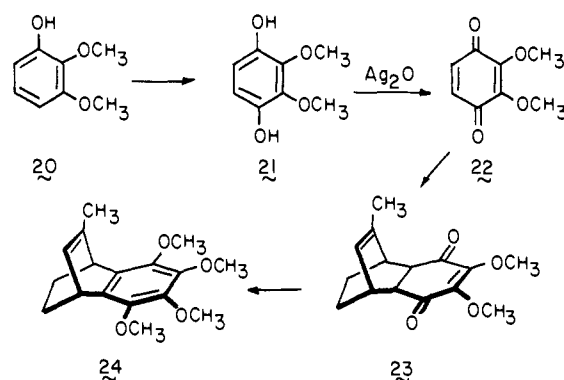
pressure hydrogenation of **9** over a palladium catalyst and direct reaction of the dihydro derivative with hydrazine hydrate in the presence of triethylamine gave the hydrazone without complications from azine formation.¹⁰ Oxidation of the hydrazone with iodine and piperidine, with a large excess of the latter reagent to deter *gem*-diiodide formation, gave **10**. When treated with lithium dimethylcuprate, **10** was converted to **2a** (60%) in addition to dimeric coupling product.

Reaction of *p*-benzoquinone with 2-methylcyclohexadiene (**11**)¹¹ in refluxing ethanol afforded adduct **12** in 57% isolated yield (Scheme II). This solid was directly O-methylated according to literature precedent.¹⁴

A particularly expedient synthesis of **2c** can be realized by the condensation of tetrafluorobenzene with **11**. Unfortunately, this approach suffers from operation of a competitive ene process which gave companion olefinic products difficultly separable from **2c**. The preferred route to the isomerically pure tetrafluoro derivative proceeded from the known ketone **13**¹⁵ via **14** in the manner discussed previously (Scheme III).

For reference purposes, it was considered desirable to have the 5,8-bis(dimethylamino) (**19**) and tetramethoxy (**23**) systems in hand. To obtain **19**, recourse was first made to the direct oxidation of **12** with Fremy's salt.¹⁶ However, only a 27% yield of the desired substituted *p*-benzoquinone **15** was obtained. Alternatively, **12** was isomerized to the hydroquinone with potassium carbonate (94% yield).^{17,18} Silver oxide oxidation^{18a,19} of this intermediate delivered **15** in a very clean and almost quantitative reaction. Its bis(oxime) **16** was not reduced with aluminum amalgam, while lithium aluminum hydride in refluxing tetrahydrofuran²⁰ gave **17a**

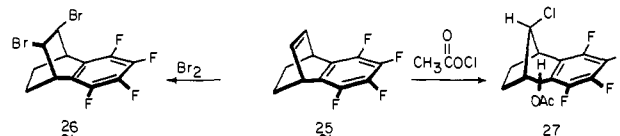
Scheme V



in low (28%) yield (Scheme IV). The preferred reagent for this conversion proved to be zinc dust in the presence of ammonia²¹ (98% yield). Completion of the sequence involved formation of the *N,N'*-diurethane,²² *N*-methylation²³ of **17b** to give **18**, and reduction with LiAlH₄.²⁴

In our hands, repetition of an earlier procedure²⁵ for obtaining 2,3-dimethoxybenzoquinone (**22**) which involved nitration of pyrogallol 1,2-dimethyl ether, reduction to the amino compound, and oxidation with ferric chloride proved problematical. The direct oxidation²⁶ of pyrogallol dimethyl ether with Fremy's salt also met with serious complications. Our ultimately successful route to **22** took advantage of potassium persulfate oxidation²⁷ of **20** to **21** followed by silver oxide oxidation (Scheme V). The further conversion of **22** to **24** proceeded straightforwardly.

Limitations on Electrophile Selection. The chemistry of benzobicyclo[2.2.2]octadienes can become plagued by skeletal rearrangements, especially as the lifetimes of the intermediate cations are increased. This phenomenon is intimately linked to the tendency of the aryl ring for Wagner-Meerwein shift, even when very electron deficient. In earlier work by Barkhash's group, who has examined selected ionic additions to the tetrafluoro derivative **25**,²⁸ reaction with bromine was found to proceed without rearrangement to give **26**. Although this reagent does not allow



analysis of which of the two competing modes of attack is preferred, its behavior contrasts markedly with that produced by "acetyl hypochlorite" (as *tert*-butyl hypochlorite in acetic acid).^{28a} In this instance, complete isomerization to **27** is observed. The propensity for skeletal rearrangement expectedly increases as the migratory ability of the aromatic moiety is enhanced such as in **2b**.²⁹ Although the stereochemistry of initial electrophilic attack can still be deduced when rearrangement occurs, one has no control over the possible intervention of phenonium ions at one end of the electronic scale but not the other. To minimize these potentially vexatious complications, we have concentrated our attention on electrophiles which are generally deemed to be weak or soft. In this manner, the original skeletal structure of the

(9) Cimarusti, C. M.; Wolinsky, J. *J. Am. Chem. Soc.* **1968**, *90*, 113.

(10) Barton, D. H. R.; O'Brien, R. E.; Sternhell, S. *J. Chem. Soc.* **1962**, 470.

(11) This diene was produced by sulfuryl chloride chlorination¹² of 2-methylcyclohexanone, dehydrochlorination with lithium chloride in DMF at 110 °C, formation of the tosylhydrazone (mp 160–163 °C) with 82% efficiency, and application of the standard Shapiro reaction.¹³

(12) Warnhoff, E. W.; Martin, D. G.; Johnson, W. S. "Organic Syntheses"; Wiley: New York, 1963; Coll. Vol. IV, p 162.

(13) Shapiro, R. H.; Heath, M. J. *J. Am. Chem. Soc.* **1967**, *89*, 5734.

(14) Meinwald, J.; Wiley, G. A. *J. Am. Chem. Soc.* **1958**, *80*, 3667.

(15) (a) Buxton, P. C.; Hales, N. J.; Hankinson, B.; Heaney, H.; Ley, S. V.; Sharma, R. P. *Chem. Soc. Perkin Trans. 1* **1974**, 2681. (b) Hales, N. J.; Heaney, H.; Ley, S. V. *Ibid.* **1974**, 2702.

(16) Powell, V. H. *Tetrahedron Lett.* **1970**, 3463.

(17) Birch, A. J.; Butler, D. N.; Sidall, J. B. *J. Chem. Soc.* **1964**, 2941.

(18) No hydroquinone was obtained when **12** was treated with HBr in acetic acid: (a) Bartlett, P. D.; Ryan, M. J.; Cohen, J. G. *J. Am. Chem. Soc.* **1942**, *64*, 2649. (b) Diels, O.; Alder, K. *Chem. Ber.* **1929**, *62*, 2337.

(19) Vaughan, W. R.; Yoshimine, M. *J. Org. Chem.* **1957**, *22*, 7.

(20) Smith, D. R.; Maienthal, M.; Tipton, J. *J. Org. Chem.* **1952**, *17*, 294.

(21) Jochims, J. C. *Monatsh. Chem.* **1963**, *94*, 679.

(22) Adams, R.; Anderson, J. L. *J. Am. Chem. Soc.* **1950**, *72*, 5154.

(23) Dannley, R. L.; Lukin, M. *J. Org. Chem.* **1957**, *22*, 268.

(24) Dannley, R. L.; Lukin, M.; Shapiro, J. *J. Org. Chem.* **1955**, *20*, 92.

(25) Baker, W.; Smith, H. A. *J. Chem. Soc.* **1931**, 2542.

(26) (a) Wehrli, P. A.; Pigott, F. *Org. Synth.* **1972**, *52*, 83. (b) Teuber, H. J.; Rau, W. *Chem. Ber.* **1953**, *86*, 1036.

(27) Baker, W.; Savage, R. I. *J. Chem. Soc.* **1938**, 1602.

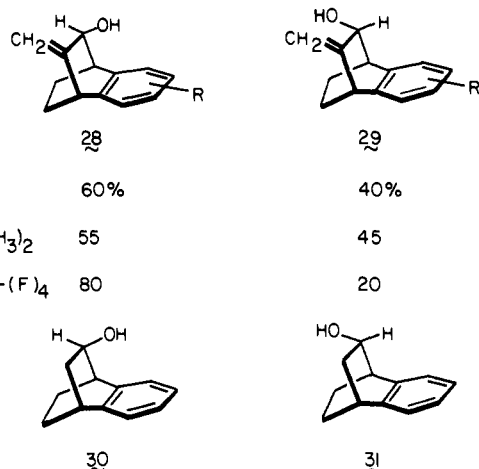
(28) (a) Povolotskaya, N. N.; Limasova, T. I.; Berus, E. I.; Exner, O.; Barkhash, V. A. *J. Org. Chem. USSR (Engl. Transl.)* **1970**, *6*, 1615. (b) Vorozhitsov, I. N.; Berus, E. I.; Derendyaev, B. G.; Barkhash, V. A. *J. Gen. Chem. USSR (Engl. Transl.)* **1969**, *39*, 2264. (c) Lobanova, T. P.; Berus, E. I.; Barkhash, V. A. *Ibid.* **1969**, *39*, 2269.

(29) Wells, G. J., unpublished findings.

substrate molecules is retained and the stereoselection observed through the series **2a–c** should be truly representative of electronic influences.

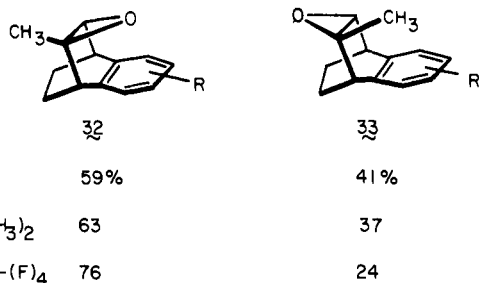
Photooxygenation. The three benzobicyclo[2.2.2]octadienes were exposed to singlet oxygen (as generated by rose bengal sensitization) in the three solvent systems acetonitrile, acetone, and methanol. Following direct reduction of the resulting allylic hydroperoxides, the distributions of allylic alcohols were determined by VPC for **2a** and **2c**. The epimeric alcohols derived from **2b** were labile under these conditions and product analysis was therefore achieved by NMR integration and preparative TLC separation. The syn/anti ratios for all three examples differed by less than 5% in the three solvents studied.

The structural assignments to **28** and **29** follow convincingly



from their spectroscopic properties. Much as with the known compounds **30** and **31**,³⁰ the syn alcohols show an infrared hydroxyl band at 3585 cm⁻¹ whereas the anti alcohols exhibit characteristic absorption in the 3605–3620-cm⁻¹ region. Additionally, the carbinol protons in **29** and **31** are shielded with respect to their counterparts in the syn alcohols. The protons on the ethano bridge also reflect the orientation of the hydroxyl group. In the anti isomers, these protons appear as a broad multiplet at δ 2.5–1.1 because of differential shifting caused by the proximal OH; for the syn isomer, this signal is narrower and much more sharply defined. Finally, the vinyl protons in **29** show long-range coupling to the carbinol hydrogen. This effect is not seen in **28** due to adoption in these systems of a dihedral angle approaching 0°.

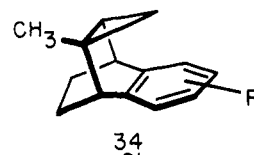
Epoxidation. Reaction of **2a–c** with *m*-chloroperbenzoic acid afforded mixtures of epoxides **32** and **33** which were easily sep-



arated by preparative TLC on basic alumina. Product stereochemistry was ascertained by comparison of the chemical shifts of the methyl groups. When positioned above an aromatic ring, such a substituent is generally shielded by approximately 15 Hz relative to one residing in the vicinity of a saturated center.³¹

Stereochemical correlation between **32a** and **33a** and their allylic alcohols (**28a** and **29a**, respectively) was accomplished by ring opening with lithium diethylamide.

Simmons–Smith Cyclopropanation. The Simmons–Smith reagent has long been recognized to behave as a weak electrophile toward double bonds.³² Thus, the reactivity of an olefin increases with increased alkyl substitution about the double bond, although the effect is somewhat offset by a concurrently enhanced steric contribution. In the case of **2a–c**, there is observed an overwhelming preference for syn attack to produce exclusively **34a–c**

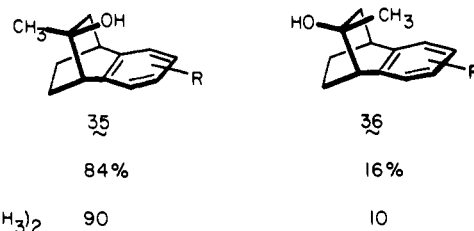


g, R = H ; **b**, R = 5,8-(OCH₃)₂ ; **c**, R = 5,6,7,8-(F)₄

within our limits of detectability. These results were foreshadowed by the work of Kitahonoki,³³ who demonstrated a 99.7% syn stereoselectivity for the parent benzobicyclo[2.2.2]octadiene.

Oxymercuration. Our objective in assessing the stereoselectivity of the oxymercuration of **2a–c** was to cleave the organomercurial reductively and examine the epimeric composition of the resulting alcohols. Consequently, it became imperative to establish whether the initial addition of mercuric acetate proceeded in a cis or trans fashion. In this connection, Cristol and Jensen had shown that mercuric acetate adds in cis fashion to dibenzobarrelene when the reaction is conducted in glacial acetic acid as solvent.³⁴ This result was evident from the cis coupling of the vicinal protons (8.5 Hz) as opposed to the known trans coupling (3.5 Hz) of these same hydrogens. Note that the presence of the methyl group in **2** precludes the use of a similar stereochemical analysis. In our hands, benzobarrelene proved to undergo cis oxymercuration in glacial acetic acid or in 50% aqueous tetrahydrofuran, the solvent system we preferred. Brown has also observed cis addition of Hg(OAc)₂ in aqueous tetrahydrofuran to various norbornenyl derivatives.³⁵

On this basis, we were confident that the stereochemistry of tertiary alcohols **35** and **36** were the end result of cis oxy-



mercuration. In situ reduction of the intermediate organomercurials with sodium borohydride proceeded uneventfully with **2a** and **2b**. In the **2c** example, however, degradative elimination to return the olefin was invariably observed. Behavior of this type had been witnessed previously.³⁶ Nonetheless, the marked preference for syn attack of this bulky reagent is clearly established in the first two examples. In order to gain additional internal consistency, epoxide **32** was reduced with lithium triethylborohydride.³⁷ Syn alcohol **35b** resulted.

Hydroboration. The stereoselection observed in the hydroboration–oxidation of **2a–c** was also predominantly syn. The minor products were easily recognized as **38** on the basis of the shielded

(32) Simmons, H. E.; Cairns, T. L.; Vladuchick, S. A.; Hoiness, C. M. *Org. React.* **1973**, *20*, 1.

(33) Kitahonoki, K.; Sakurai, S.; Tori, K.; Veyama, M. *Tetrahedron Lett.* **1976**, 263.

(34) Cristol, S. J.; Jensen, F. R.; Muller, J. J.; Beckley, R. S. *J. Org. Chem.* **1972**, *37*, 4341.

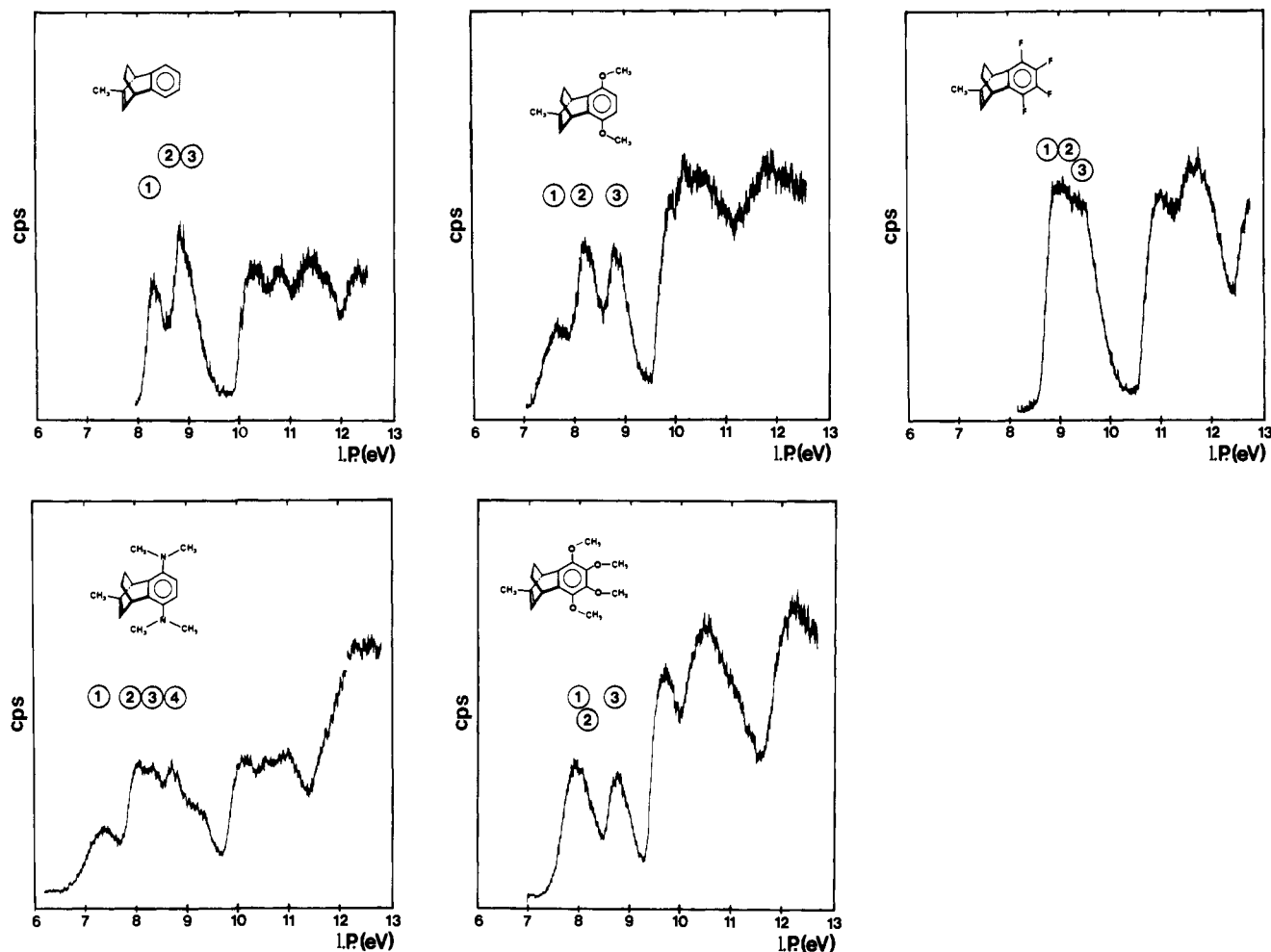
(35) Brown, H. C.; Kawakami, J. H. *J. Am. Chem. Soc.* **1973**, *95*, 8665.

(36) Coxon, J. M.; Hartshorn, M. P.; Lewis, A. J. *Tetrahedron* **1970**, *26*, 3755.

(37) (a) Brown, H. C.; Schubert, R. M.; Krishnamurthy, S. *J. Am. Chem. Soc.* **1973**, *95*, 8486. (b) Brown, H. C.; Krishnamurthy, K. *Ibid.* **1973**, *95*, 1669.

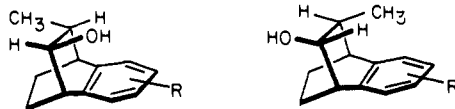
(30) (a) Tori, K.; Takano, Y.; Kitahonoki, K. *Chem. Ber.* **1964**, *97*, 2798. (b) Kitahonoki, K.; Takano, Y. *Tetrahedron Lett.* **1963**, 1597.

(31) Tori, K.; Kitahonoki, K.; Takano, Y.; Tanida, H.; Tsuji, T. *Tetrahedron Lett.* **1964**, 559.

Figure 1. He I photoelectron spectra of **2a-c**, **19**, and **24**.Table I. Relative Rates of Electrophilic Additions to **2a-c**

reagent	2a	2b	2c
$^1\text{O}_2$	0.81	9.08	1.00
MCPBA	3.00	3.36	1.00
$\text{Et}_2\text{Zn}/\text{CH}_2\text{I}_2$	5.07	18.0	1.00
$\text{Hg}(\text{OAc})_2$	1.27	1.04	1.00
B_2H_6	0.95	0.97	1.00

nature of their methyl doublets (δ 0.8–0.7) relative to those for **37** (ca. 1.20).



g , R = H	67%	33%
b , R = 5,8-(OCH ₃) ₂	75	25
c , R = 5,6,7,8-(F) ₄	94	6

Comparative Rate Studies. Rate constants for the photooxygenation of **2a-c** were obtained by laser pulse radiolysis techniques at the Center for Fast Kinetic Research, Austin, TX.³⁸ The rates (0.545×10^{-5} , 6.12×10^{-5} , and 0.674×10^{-5} L mol⁻¹ s⁻¹, respectively) reveal that electronic factors contribute little in the way of kinetic inequalities. The same conclusion was arrived at for the other processes by obtaining relative rates. The method

(38) We thank Dr. M. A. J. Rodgers and Dr. Larry Hertel for the acquisition of these data.

Table II. Comparison between Measured Vertical Ionization Potentials ($I_{V,J}$) and Calculated Orbital Energies (ϵ_J) (all values in eV)

compd	peak	$I_{V,J}$	assign ^a	ϵ_J (MINDO/3) ^b
2a	1	8.33	πS^{B}	8.68
	2	8.80	πA^{B}	8.98
	3	8.94	πS^{D}	9.23
2b	1	7.70	πA^{B}	7.99
	2	8.20	πS^{B}	8.91
	3	8.80	πS^{D}	9.25
19	1	7.34	$n/\pi\text{A}^{\text{B}}$ AB	7.07
	2	8.04	πS^{B}	8.60
	3	8.26	n_+	9.37
	4	8.68	πS^{D}	9.16
24	1	8.85	πA^{B}	8.57
	2	8.85	πS^{B}	8.68
	3	8.64	πS^{D}	9.37
2c	1	8.94	πA^{B}	9.18
	2	9.08	πS^{B}	9.36
	3	9.36	πS^{D}	9.91

^a B = benzene, D = double bond, S = symmetric, A = antisymmetric, AB = antibonding. ^b All calculations were performed without the methyl group at the octadiene double bond. In the case of **21**, OH groups have been used instead of methoxy substituents.

consisted of allowing two of the three substrates to vie for 0.4 equiv of the electrophile in question and determining the ratio of unreacted starting materials by VPC through implementation of the internal standard technique. The results are compiled in Table I.

In all cases save one (which is not significantly astray), the relative rates are of the same order of magnitude in progressing

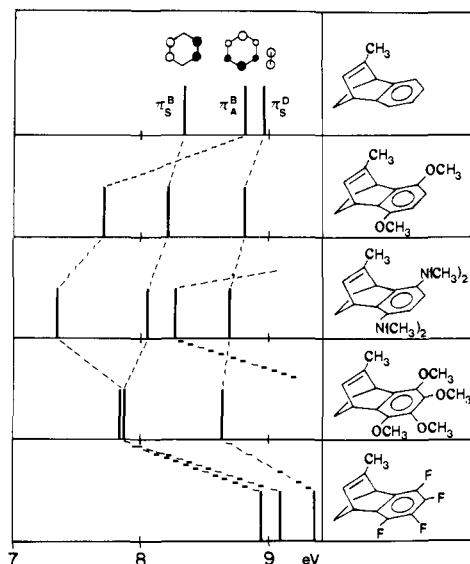
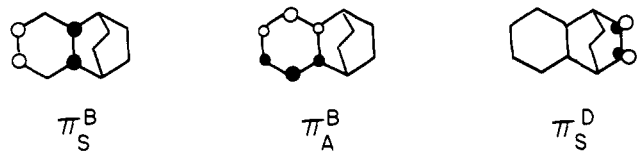


Figure 2. Correlation between the first PE bands of the benzobicyclo[2.2.2]octadienes.

from **2a** to **2c**, indicative that progressive electronic changes about the aromatic ring hardly affect the reactivity of the olefinic π orbital.

Photoelectron Spectroscopy Studies and Theoretical Calculations. To permit rationalization of the stereochemical preferences witnessed above, we have investigated the He I photoelectron (PE) spectra of the relevant molecules as well as those of **19** and **24**. The measured ionization potentials have been compared with computational results of the MINDO/3 type³⁹ on the assumption that Koopmans' theorem ($I_{V_j} = -\epsilon_j$)⁴¹ is applicable. The behavior and shape of the frontier orbitals in the benzobicyclo[2.2.2]octadiene series are also analyzed by means of MO wave functions as likewise derived by MINDO/3 calculations.

The relevant PE spectra are shown in Figure 1; the vertical ionization potentials together with their assignment and the calculated IP's are collected in Table II, while a graphical correlation of the IP's is displayed in Figure 2. The PE spectrum of hydrocarbon **2a** exhibits two maxima below 10 eV at 8.33 and 8.80 eV; however, a shoulder can be found at 8.94 eV on the high-energy side of the second band. On the basis of earlier PE spectroscopic investigations on benzonorbornadienes⁴² and 9-isopropylidenebenzonorbornenes,^{1,3} the first peak can be confidently assigned to an ionization event from the symmetric π MO of the benzene moiety (π_S^B). The second broad band, which



contains two ionization events, is due to electronic ejection out of the antisymmetric π_A^B MO of the aromatic ring and the π orbital of the isolated double bond (π_S^D). The PE spectra of various benzonorbornadienes⁴² and their 7-isopropylidene derivatives^{1,3} support an assignment of π_A^B above π_S^D , a conclusion also derivable within the MINDO/3 framework. In the present MINDO/3 calculations where complete geometry optimization was used, the olefinic methyl substituent was omitted to lessen the consumption of computer time.

The methoxy substituents in **2b** and the dimethylamino groups in **19** should primarily destabilize the π_A^B linear combination, while

their influence upon π_S^B and π_S^D should be of minor importance. This is clearly observed. The first band of **2b** which appears at 7.70 eV is due to π_S^B and the third maximum at 8.80 eV to π_S^D . Thus, π_A^B has been destabilized by 1.10 eV as a consequence of its methoxyl groups. On the other hand, only a small destabilization of about 0.14 eV is found for the two remaining π orbitals in the outer valence region. Once again, there exists good agreement between the measured IP's and the MINDO/3 results. A further lowering of the first ionization potentials is observed in the case of bis(dimethylamino) derivative **19** where I_{V_1} is found at 7.34 eV. The remaining maxima at 8.04, 8.26, and 8.68 eV in the lower energy region are part of a series of strongly overlapping bands. The first peak must, of course, be assigned to a MO of S symmetry, viz. the antibonding linear combination between the n lone-pair combination of the dimethylamino substituents and π_A^B of the benzene ring.⁴³ Maximum 2 is identified as the symmetric π orbital of the six-membered ring π_S^B , and the third component of the band system corresponds to an ionization event from the n_+ lone-pair combination. The fourth maximum is assigned to the ethylene bridge. This sequencing is in line with the observed shifts of the PE bands in the series **2a-c** and corresponds nicely with the results of Maier and Turner for aniline derivatives.⁴⁴ Since the $N(\text{CH}_3)_2$ groups have been replaced by NH_2 functions in our MINDO/3 calculations, the methyl-induced destabilization of the nitrogen lone pairs is missing and the theoretical procedure therefore fails to predict accurately the sequence of ionization events.

Tetrasubstitution of the benzene ring also influences the symmetric π combination which has nodes in the positions α to the bridging carbon atoms. In the PE spectrum of **24**, two overlapping bands with a center of gravity at 7.85 eV are observed on top of a single peak with a maximum at 8.64 eV corresponding to the ethylene bridge. Thus, the π MO's of the benzene ring must be responsible for the first two ionization events. Due to steric hindrance between the methoxy groups, an in-plane orientation of the OCH_3 substituents is not possible. Therefore, the MINDO/3 results of Table II have been obtained at a geometry where all four methoxyls are rotated by 90° out of the π plane. In accordance with the experimental data, MINDO/3 predicts a negligible energy gap of 0.11 eV between π_A^B and π_S^B . Additionally, the separation to the π_S^D MO is calculated to be 0.75 eV, a value close to the measured difference of 0.79 eV between the center of gravity of π_A^B/π_S^B and π_S^D .

In tetrafluoro derivative **2c**, only one broad band is found in the outer valence region. The estimated maxima of this system are located at 8.94, 9.08, and 9.36 eV as shoulders on the high-energy side of the band system. The first two components are assigned to the two MO's related to the aromatic ring (π_A^B and π_S^B), while the third maximum should have its origin in the π MO of the ethylene bridge. As Table I indicates, this interpretation is supported by the MINDO/3 calculations.

The PE spectra in the lower energy region of the benzobicyclo[2.2.2]octadienes agree in so far as the two MO's derived from the benzene system (π_S^B and π_A^B , respectively) are always found on top of the π MO of the ethylene bridge (π_S^D). The relative ordering of the π_S^B/π_A^B pair clearly depends on the substituents attached to the benzene moiety. In the case of **2a**, π_S^B is found above π_A^B , while the opposite is encountered in the dimethoxy and bis(dimethylamino) derivatives. The remarkable separation between π_S^B and π_A^B exhibited by the latter two compounds is reduced if two additional substituents occupy the β centers with respect to the bridging fragment (C_6 , C_7). In the tetramethoxy compound, only one peak is found for the π pair, while two strongly overlapping bands are observed for the tetrafluoro derivative. As shown in Table II, the MINDO/3 ordering of the ionization processes is in line with the experimental findings for **2a-c**. Consequently, these calculations serve as a tool suitable for analysis of the MO properties of the benzobicyclo[2.2.2]oc-

(39) Bingham, R. C.; Dewar, M. J. S.; Lo, D. H. *J. Am. Chem. Soc.* **1975**, *97*, 1285.

(40) Bischof, P. *J. Am. Chem. Soc.* **1976**, *98*, 6844.

(41) Koopmans, T. *Physica (Utrecht)* **1934**, *1*, 104.

(42) Haselbach, E.; Rossi, M. *Helv. Chim. Acta* **1976**, *59*, 278.

(43) Maier, J. P. *Helv. Chim. Acta* **1974**, *57*, 994.

(44) Maier, J. P.; Turner, D. W. *J. Chem. Soc., Faraday Trans. 2* **1973**, *69*, 521.

Table III. Summary of syn/anti Ratios for Various Electrophilic Additions to 2a-c

compd	$^1\text{O}_2$	MCPBA	B_3H_6	$\text{Hg}(\text{OAc})_2$	$\text{Et}_2\text{Zn}/\text{CH}_2\text{I}_2$
2a	60/40	59/41	67/33	84/16	100/0
2b	55/45	63/37	75/25	90/10	100/0
2c	80/20	76/24	94/6		100/0

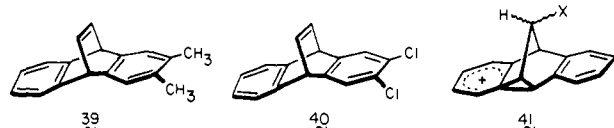
tadienes and potentially their stereochemical behavior toward electrophiles.

Discussion

In principle, at least five factors can be identified that might determine the stereochemical course of electrophilic attack in the series 2a-c: (a) a steric factor caused by the hydrogen atoms of the ethano bridge that promotes kinetically favored attack by an incoming electrophile on the syn surface of the π bond; (b) an energetically favorable phase relation in the frontier orbitals of S symmetry which arises as the direct result of through-space coupling⁴⁵ between the two π units; (c) some modification of the properties of the two halves of the ethylenic π lobes as a result of through-bond coupling⁴⁵ via the benzobicyclo[2.2.2]octadiene σ framework that leads to different activation energies for syn and anti attack; (d) favorable long-range Coulomb interaction between the aromatic segment and a fragment of the attacking electrophile; (e) a directive influence involving some type of charge-transfer interaction between the valence electrons of the aromatic ring and the electrophilic reaction partner.

There is no question that the hydrogen atoms of the ethano bridge can provide sufficient bulk to divert an incoming electrophile preferentially away from the anti face in favor of the somewhat less encumbered syn face of the double bond. In fact, the argument can be advanced that progressively larger electrophiles provide correspondingly higher syn/anti ratios (Table III). However, this effect is clearly not overwhelming. Steric barriers of this magnitude are readily overcome by long-range homoconjugative stabilization in 9-isopropylidenebenzonorbornenes,^{1,3} although allowances must be made for the change in relative orientation of the π bond between the two systems. A certainty is that steric forces cannot be the basis for the different stereoselectivities which a single reagent displays as it acts on 2a, 2b, and 2c. These effects, which are most evident with the first three reagents cited in Table III, must arise from electronic factors. The somewhat unfortunate aspect of these developments is that the kinetically favored syn attack which is observed is no longer contrasteric as it is with 9-isopropylidenebenzonorbornenes and the range of stereoselectivity effects is correspondingly compressed.

Cristol and Kochansky have studied the stereoselectivities of electrophilic attack upon the unsymmetrical dibenzobarrelenes 39 and 40.⁴⁶ No preference for either face of the double bond



was noted for diborane, benzenesulfonyl chloride, or mercuric acetate. On the other hand, bromine, chlorine, hydrogen bromide, and acetic acid showed directional effects, with electrophilic attack being preferred at the side anti to the dimethyl substituted ring of 39 and syn to the dichloro substituted ring of 40. The latter results were rationalized as involving participation in the transition state of the more electron-rich aromatic ring as in 41. While rearrangements were purposefully avoided in the present work, the response of 39 and 40 to weak electrophiles signals that the electronic contributions to which we refer in 2a-c must arise from

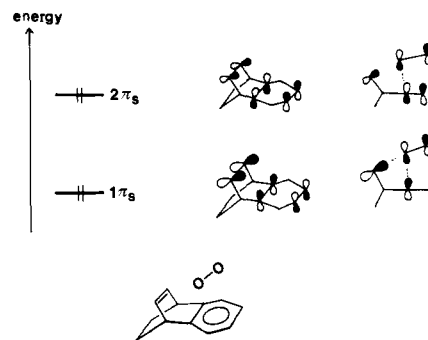


Figure 3. Possible linear combinations for $\pi_S^B \pm \pi_S^D$ if through-space interaction between them is important. At the right side, the phase relation between a π^* orbital of O_2 and $1\pi_s$, as well as a $2\pi_s$, is indicated.

the enormously different orbital construction of an ethano bridge and substituted aromatic ring.

In this connection, however, the involvement of through-space interaction between the π moieties cannot be of major importance in determining the observed product ratios. With benzenorbornadiene derivatives,^{42,47} the stereochemical preferences observed in Diels-Alder additions have been traced back to a destabilization of the transition state due to out-of-phase coupling between the π fragments by means of a through-space mechanism on one side and the incoming diene on the other. If the assumption is made that through-space interaction between the two π units in 2a-c is significant, then the corresponding wave functions should show the behavior displayed in Figure 3. For the upper linear combination $2\pi_s$, which is characterized by predominant participation of the benzenoid π system and smaller contributions from the ethylene bridge, a node is seen between the two π units. In the case of the lower energy linear combination ($1\pi_s$), the moieties are in phase. The interaction between this pair of occupied substrate MO's and the acceptor levels of an incoming electrophile importantly operates in different directions. For $2\pi_s$, the alternation in phase relations leads to a destabilizing component in the interaction, while the opposite is found for $1\pi_s$, where in-phase interaction occurs between the three participating fragments. As both effects should be closely comparable in magnitude, no net modification of the transition state is expected.

The preceding argumentation is valid only if there exists efficient through-space coupling in benzobicyclo[2.2.2]octadiene derivatives. To resolve this question, we have analyzed the wave functions of the MO's with predominant participation of the π bridge. A plot of the corresponding MO's recorded in the symmetry plane is shown in Figure 4. The molecular wave functions clearly demonstrate that coupling between the two π units is absent in these systems. On the other hand, significant contributions to the MO's materialize on the σ ribbon as the result of through-bond interaction in these π/σ nonorthogonal species. Consequently, the two lobes of the canonical π_S^D MO are different.^{48,49} This phenomenon is particularly evident in Figure 4 where enlarged π densities are seen syn to the benzene ring in 2a and 2b. In the tetrafluoro example (2c), both halves are equivalent, indicating a lack of orbital directionality for electrophilic attack.

An inspection of the LCAO wave function of π_S^D in the case of 2a and 2b shows the enhanced π contribution on the syn face to be the result of a disrotatory motion of the π lobes in a fashion that decreases the distance vector between the two lobes syn to the six-membered ring π fragment (Figure 5). In recent publications, we have explained in some detail the origin of π deformations which exist in the canonical MO's of nonorthogonal π/σ systems.^{48,49} The canonical π orbital of the ethylene bridge, $\phi_{S(\pi)}^{\text{CMO}}$, can be expressed in terms of a pure localized π orbital

(47) Pfaendler, H. R.; Tanida, H.; Haselbach, E. *Helv. Chim. Acta* 1974, 57, 383.

(45) (a) Hoffmann, R.; Imamura, A.; Hehre, W. J. *J. Am. Chem. Soc.* 1968, 90, 1499. (b) Hoffmann, R. *Acc. Chem. Res.* 1971, 4, 1. Gleiter, R. *Angew. Chem.* 1974, 86, 770.

(46) Cristol, S. J.; Kochansky, M. C. *J. Org. Chem.* 1975, 40, 2171.

(48) (a) Paquette, L. A.; Carr, R. V. C.; Böhm, M. C.; Gleiter, R. *J. Am. Chem. Soc.* 1980, 102, 1186. (b) Böhm, M. C.; Carr, R. V. C.; Gleiter, R.; Paquette, L. A. *Ibid.* 1980, 102, 7218.

(49) Böhm, M. C.; Gleiter, R. *Tetrahedron*, in press.

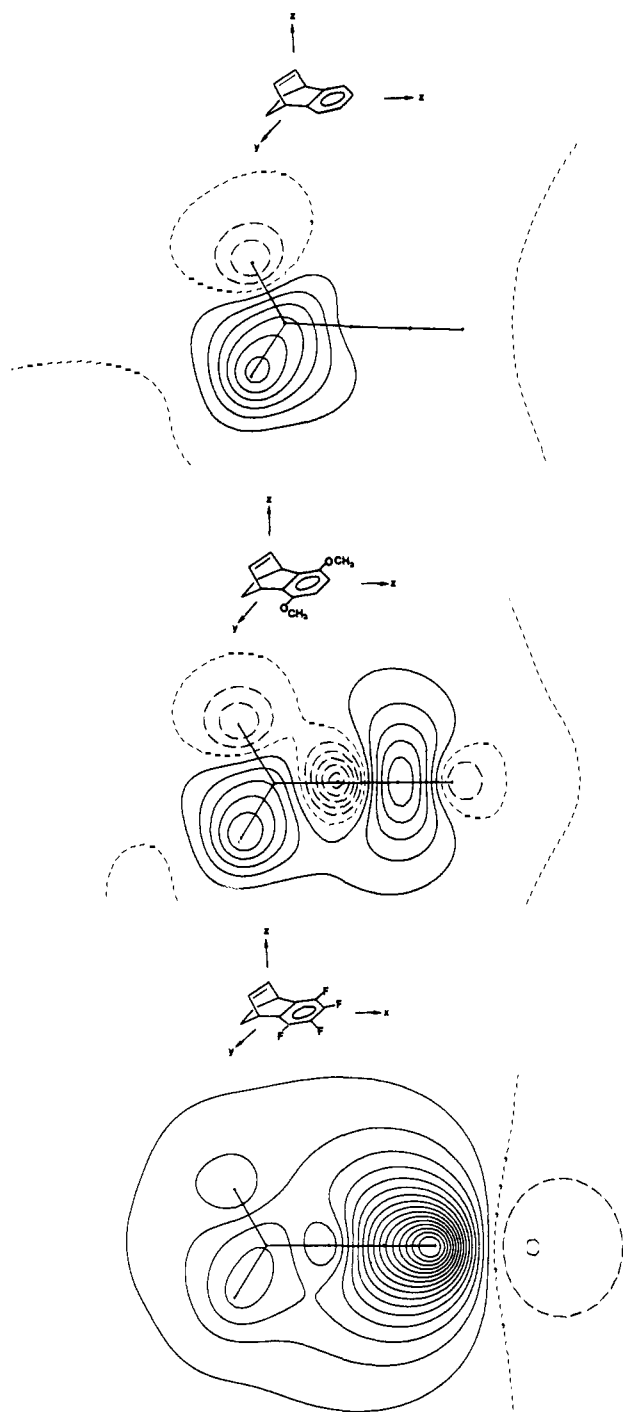


Figure 4. Contour diagrams of the calculated electrostatic potentials of **2a-c** (without the CH_3 groups). The maps are drawn in the x,y plane and the intervals between the contours is 5 kcal/mol.

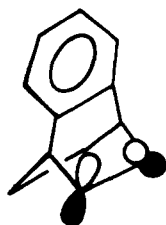


Figure 5. Rotation of the π lobes of the double bond in response to interaction with the σ framework.

without contribution of the σ frame ($\phi_{S(i)}^{\text{LMO}}$) plus the contributions of so called precanonical σ -ribbon orbitals ($\phi_{S(i)}^{\text{PCMO}}$); the latter is a one-electron set delocalized over the whole molecule

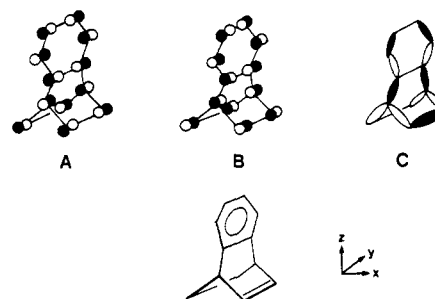


Figure 6. Precanonical σ orbitals of **2a** which interact predominantly with the localized π orbital. For the sake of clarity in A and B, only AO representations have been chosen.

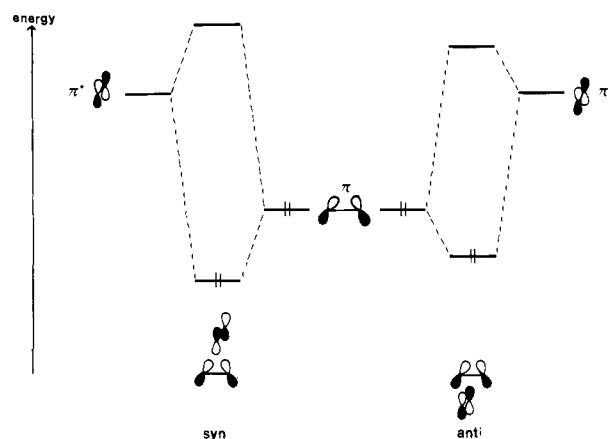


Figure 7. Stabilization of the π orbital of the double bond in benzo-bicyclo[2.2.2]octadienes as the result of interaction with π^* in a symmetrical manner for a syn (left) and anti (right) approach.

containing the averaged influence of the remaining $(N - 2)$ one-electron functions but missing $\phi_{S(\pi)}^{\text{LMO}}$.⁵⁰ In eq 1, the nu-

$$\phi_{S(\pi)}^{\text{CMO}} = \phi_{S(\pi)}^{\text{LMO}} + \sum_i \frac{(F\phi_{S(\pi)}^{\text{LMO}})(F\phi_{S(i)}^{\text{PCMO}})}{(F\phi_{S(\pi)}^{\text{LMO}})(F\phi_{S(\pi)}^{\text{LMO}}) - (F\phi_{S(i)}^{\text{PCMO}})(F\phi_{S(i)}^{\text{PCMO}})} \phi_{S(i)}^{\text{PCMO}} \quad (1)$$

merator has the function of a through-bond type coupling constant which determines the shape of the canonical MO. In the denominator of the perturbation expansion, the self-energies of the localized MO ($\phi_{S(\pi)}^{\text{LMO}}$) and the ensemble of the precanonical σ set ($\phi_{S(i)}^{\text{PCMO}}$) determine the degree of σ/π interaction as a function of the basis energies of the various one-electron fragments. Within the computational framework of MINDO/3, at least three PCMO's of σ -type can be identified that interact with the localized π MO. The relevant σ combinations are displayed in Figure 6. MO's A and B are closely related to Hoffmann's SS type σ -ribbon orbitals⁵¹ with maximal localization in the y axis. C, on the other hand, shows predominant localization at those bridging carbon atoms which connect the double bond, ethano bridge, and benzene fragment. The contribution of the symmetric π component of the 6π moiety to the canonical $\phi_{S(\pi)}^{\text{CMO}}$ MO is small in comparison to the coupling with A, B, and C. In these terms, the preference for syn attack exhibited by benzo-bicyclo[2.2.2]octadiene **2a** and its dimethoxy derivative **2b** can be shown to have an electronic basis. Rotation of the π lobes in this fashion makes possible more efficient interaction between the π donor and the acceptor orbital of the attacking electrophile in the symmetric transition state^{52,53} on the syn face. Simultaneously, the stabilizing donor-acceptor

(50) Heilbronner, E.; Schmelzer, A. *Helv. Chim. Acta* **1975**, *58*, 936.

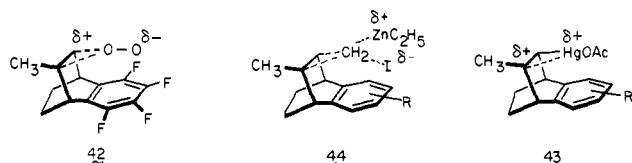
(51) Hoffmann, R.; Mollère, P. D.; Heilbronner, E. *J. Am. Chem. Soc.* **1975**, *95*, 4860.

(52) (a) Klopman, G. *J. Am. Chem. Soc.* **1967**, *90*, 223. (b) Klopman, G.; Hudson, R. F. *Theor. Chim. Acta* **1967**, *8*, 165. (c) Hudson, R. F.; Klopman, G. *Tetrahedron Lett.* **1967**, 1103.

(53) Scrocco, E.; Tomasi, J. *Fortschr. Chem. Forsch.* **1973**, *42*, 95.

interaction is reduced for anti attack due to π rotation away from the bonding region. This behavior is displayed graphically in Figure 7 for $^1\text{O}_2$ attack,^{52,53} but the argumentation can also be validly applied to the other electrophiles. However, this analysis does not hold for **2c** where no inequivalence of the π lobes can be detected. To test the validity of the MINDO/3 results, we have also performed MO calculations with current semiempirical models (EHT, CNDO, INDO). The results were invariably the same, viz., that π/σ interaction is of minor importance in **2c**. Therefore, the strong preference shown by the tetrafluoro derivative for syn attack must have a different origin.

As derived in a perturbational model by Hudson and Klopman,⁵² the contribution of the covalent interaction between the frontier orbitals is reduced if "hard" species with highly charged centers are involved in a reaction. Under these conditions, the relevant factor that determines the activation energy is the electrostatic Coulomb interaction between the active sites. Recently, we have shown that this electrostatic contribution to activation energy can be displayed if the electrostatic potential⁵³ of the reactants is analyzed.^{54,55} The MINDO/3-based electrostatic potential fields (EPF) of **2a-c** are shown in Figure 8. The approximations employed to calculate these quantities are discussed in detail elsewhere.⁵⁴ To correspond to the MO plots in Figure 4, the mirror plane has again been used as reference. The EPF representations in Figure 8 indicate that a large positive EPF distribution is found on the side of the benzene moiety in **2c**, as the electron-accepting fluorine substituents create a significant electron deficiency at the carbon atoms of the aromatic ring. Therefore, the charge separation in the highly polar peroxirane transition state, for example, may be significantly facilitated for syn attack as the trailing negative oxygen atom becomes stabilized by the positive EPF of the fluorine substituted unit (see **42**). No



comparable long-range electrostatic interaction can operate during anti attack. As shown in Figure 8, the magnitude of the EPF created in the region of the benzene moiety is reduced in the series **2c** > **2b** > **2a** as the charge separation in the benzenoid fragment is diminished. On the other hand, stronger electrostatic interactions are expected in the case of $\text{Hg}(\text{OAc})_2$ and the Simons-Smith reagent where intermediates such as **43**⁵⁶ and **44**³² are probably involved. The somewhat higher reaction rate of **2b** with the latter reagent can be understood in terms of the usual oxygen-coordinating property of $\text{Zn}(\text{II})$.

The extent of interaction in **2a** and **2b** may also be sufficient to stabilize the syn transition state in this fashion. However, we cannot rule out the involvement of a π -complex exhibiting charge transfer between both groups. Importantly, the two types of interaction to which we refer must be carefully discriminated. Whereas charge distribution is conserved in the case of electrostatic Coulomb interaction, electron transfer from one moiety to the other does intervene when a true CT intermediate is formed.

Summary

It is clear from the obvious preference for syn attack on **2a-c** that homoconjugative interaction between the olefinic π bond and aromatic ring, if operational at all, is not capable of dictating stereoselectivity. Accordingly, the results contrast strikingly with the stereochemical course of electrophilic additions to 9-isopropylidenebenzonorbornenes.^{1,3} The ethano hydrogens do introduce a steric bias into the benzobicyclo[2.2.2]octadiene framework with which the approaching reagents must deal. However, the barrier is not insurmountable and is certainly not

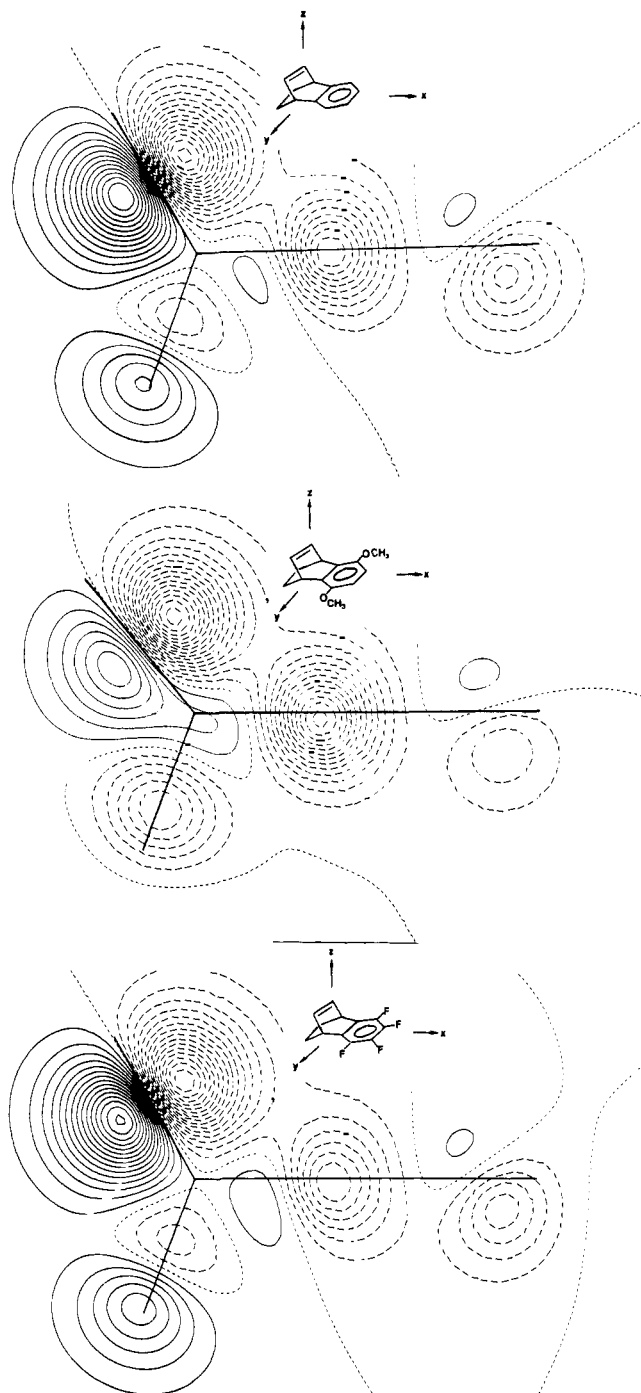


Figure 8. Plots of the olefinic π MO's of **2a-c** (without the CH_3 group). The maps are drawn in the x,z plane and the intervals between the contours are 0.01 kcal/mol.

the source of the variable stereoselectivity ratios exhibited by a given reagent, although the total available stereoselectivity range is thereby compressed. Of the various possible electronic factors which may cause syn attack to be kinetically attractive, through-space coupling between the π units can be shown to be absent. However, through-bond coupling in **2a** and **2b** does lead to disrotation of the olefinic π lobes (syn compression; anti expansion). More efficient interaction with the acceptor orbital of an electrophile can consequently develop on the syn surface. Due to the presence of the fluorine atoms, this phenomenon does not manifest itself in **2**. The high propensity of this derivative for syn attack may lie in long-range Coulomb (or charge-transfer interaction) between the aromatic ring and the attacking electrophile which is greatest in this instance. Notwithstanding the actual cause, the present stereoselectivity ratios do signal that remote

(54) Böhm, M. C.; Gleiter, R. *Tetrahedron*, in press.

(55) Gleiter, R.; Ginsburg, D. *Pure Appl. Chem.* **1979**, *51*, 1301.

(56) Bach, R. D.; Henneke, H. F. *J. Am. Chem. Soc.* **1970**, *92*, 5589.

electronic changes can duly affect the disposition of a nonconjugated double bond in its chemical reactions.

Experimental Section

Infrared spectra were recorded on a Perkin-Elmer Model 467 spectrophotometer. The ^1H NMR spectra were determined with Varian T-60 and EM-360 spectrometers, and apparent splittings are given in all cases. Mass spectra were measured with an AEI-MS9 spectrometer at an ionizing energy of 70 eV. Microanalytical determinations were made at the Scandinavian Microanalytical Laboratory, Herlev, Denmark.

2-Keto-1,2,3,4-tetrahydronaphthalene Hydrazone. In a Parr hydrogenation bottle was placed 6.60 g (38.8 mmol) of **9** dissolved in 100 mL of absolute ethanol containing 0.5 g of 5% Pd on charcoal. The system was shaken at 50 psi of hydrogen at 25 °C for 4 h. Filtration through Celite and evaporation of solvent gave 6.66 g of the dihydro derivative as a clear, slightly yellow oil which was used without further purification; ^1H NMR (CDCl_3) δ 7.15 (s, 4 H), 3.55–3.35 (m, 3 H), 2.25–1.60 (m, 7 H).

In a 250-mL round-bottom flask was placed 6.66 g (38.8 mmol) of the ketone dissolved in 80 mL of absolute ethanol, 30 mL of triethylamine, and 30 mL of hydrazine hydrate. The solution was refluxed for 2 h, cooled, poured into a 1-L Erlenmeyer flask containing 500 mL of water, and allowed to crystallize overnight at 0 °C. Filtration followed by drying under vacuum gave 6.30 g (86.7%) of hydrazone as white needles: mp 80–83 °C; ^1H NMR (CDCl_3) δ 7.1 (s, 4 H), 4.6 (br s, 2 H), 3.6 and 3.3 (2 s, 2 H), 2.2–1.7 (m, 6 H).

1,4-Dihydro-1,4-ethano-2-iodonaphthalene (10). In a 250-mL round-bottom flask fitted with an addition funnel surmounted with a drying tube was placed 6.30 g (34 mmol) of the hydrazone dissolved in a mixture of 60 mL of dry distilled piperidine and 50 mL of anhydrous tetrahydrofuran. The solution was stirred magnetically while flushed with oxygen-free nitrogen for 10 min and cooled to 0 °C, whereupon iodine (21.5 g, 85 mmol) dissolved in 70 mL of dry tetrahydrofuran was added dropwise via the addition funnel. After being stirred for 1 h at room temperature, the solution was poured into 500 mL of ice water. The organic phase was extracted into ether (4 \times 100 mL), washed with 2 N hydrochloric acid (4 \times 50 mL), water (2 \times 50 mL), 10% sodium sulfite solution (50 mL), water (50 mL), saturated sodium bicarbonate solution (50 mL), and finally water (50 mL). The ether phase was dried, filtered, and concentrated to give 8.45 g of a brown oil which solidified under vacuum.

This crude product was chromatographed on 300 g of Florisil (elution with 85% hexane/15% ethyl acetate). As the initial light yellow fractions (20 mL) were collected, they were seen to change to a light pink color, evidently the result of light-induced generation of iodine. Since the separation by analytical TLC was very good, only one large (1.5 L) fraction was collected while the entire assembly was covered by foil. Evaporation of solvent gave 6.95 g (72%) of **10** as a pale yellow solid: mp 72–73 °C; ^1H NMR (CDCl_3) δ 7.05 (s, 4 H), 6.85–6.70 (d of d, J = 7 and 2 Hz, 1 H), 4.10 (br s, 1 H), 3.80 (m, 1 H), 1.80–1.25 (m, 4 H); m/e calcd 281.9907, obsd 281.9913.

1,4-Dihydro-1,4-ethano-2-methylnaphthalene (2a). In a dry 2-L round-bottom flask was placed 24 g (126 mmol) of cuprous iodide and 750 mL of dry ether. The mixture was flushed with nitrogen, cooled to 0 °C, and stirred while 5.50 g (250 mmol, 143 mL of a 1.75 M solution in ether) of methylolithium was added via syringe. The yellow-green solution was stirred for 30 min, whereupon a solution of 6.95 g (25 mmol) of **10** in 200 mL of dry ether was added via syringe. The solution was stirred at 0 °C and slowly allowed to come to ambient temperature during 22 h before being returned to 0 °C and slowly treated dropwise with 100 mL of water. The resulting dark mixture was filtered through Celite, the ether phase was separated, and the aqueous phase was extracted with ether (4 \times 100 mL). The combined ether phases were dried, filtered, and concentrated to give 3.83 g of a yellow semi-solid. Chromatography over 150 g of silica gel (hexane elution) gave 2.55 g (60%) of **2a** as a clear oil: ^1H NMR (CDCl_3) δ 7.10 (s, 4 H), 6.00 (m, 1 H), 3.8–3.6 (m, 2 H), 1.8 (d, J = 1.5 Hz, 3 H), 1.6–1.2 (m, 4 H); m/e calcd 170.1095, obsd 170.1099.

Anal. Calcd for $\text{C}_{13}\text{H}_{14}$: C, 91.71; H, 8.29. Found: C, 91.37; H, 8.23.

A second product (2.3 g, 30%), mp 201–206 °C (dec), believed to be a dimer could also be obtained by increasing the polarity of the solvent to 10% ether/90% hexane or through crystallization of the crude product from ether: ^1H NMR (CDCl_3) δ 7.1 (br s, 8 H), 6.6–6.5 (m, 2 H), 4.2–4.0 (m, 4 H), 1.5 (m, 8 H); m/e calcd 310, 311, 312.

2-Methyl-1,3-cyclohexadiene (11). In a 500-mL Erlenmeyer flask was placed 170 mL of absolute methanol and, with slight warming, 42.82 g (0.23 mol) of tosylhydrazine was dissolved therein. With stirring, a solution of 25.00 g (0.227 mol) of 2-methylcyclohexenone in 25 mL of the same solvent was added. The solution was stirred for 30 min, stored

overnight at 25 °C, cooled to 0 °C for 1 h, and suction filtered to give 52.04 g (82.4%) of white crystals, mp 161–163 °C, after washing with 50 mL of cold methanol.

In a dry 1-L three-necked round-bottom flask flushed with nitrogen and equipped with an overhead stirrer was placed 300 mL of dry ether and 63.55 g (0.228 mol) of the above tosylhydrazine. The solution was stirred while cooling to –40 °C (chlorobenzene/dry ice). Added to this solution via syringe was 230 mL of a 2 N solution of $\text{CH}_3\text{Li-LiBr}$ complex in ether (0.457 mol) in 25-mL aliquots over 2 h. The yellow solution was stirred at –40 °C for a short while and allowed to warm to room temperature. The reaction mixture was cooled to 0 °C and 50 mL of water was added. The precipitated solids were separated by filtration and washed with ether. The combined ether phases were separated from the aqueous layer and washed with saturated ammonium chloride solution (2 \times 50 mL). The aqueous layer was extracted with ether (2 \times 35 mL), and the combined ether phases were dried. The ether was removed by distillation through a Vigreux column and the product exhibited a boiling point of 104–107 °C: yield 9.03 g (42%) of colorless liquid; ^1H NMR (CDCl_3) δ 5.75 (s, 2 H), 5.40 (s, 1 H), 2.10 (s, 4 H), 1.70 (s, 3 H).

1,4-Dihydro-1,4-ethano-2-methyl-5,8-dimethoxynaphthalene (2b). In a 25-mL round-bottom flask was placed a suspension of *p*-benzoquinone (3.44 g, 0.032 mol) in 100 mL of absolute ethanol. The solution was rapidly stirred while 3.00 g (0.032 mol) of **11** was added. The stirred solution was refluxed for 3 h, cooled and allowed to crystallize overnight at room temperature. Filtration and washing with cold ethanol (20 mL) gave 2.04 g of greenish yellow crystals. Concentration of the mother liquors to 10 mL followed by cooling to 0 °C for 6 h provided another 1.40 g of yellow crystals. Recrystallization of these combined crops from 12 mL of ethanol at 25 °C overnight gave 2.26 g of **12** as dull yellow needles, mp 81–82 °C. The mother liquors provided two additional crops of 1.20 and 0.22 g, mp 80–82 °C and 80.5–82.5 °C, respectively. Total yield: 3.68 g (56.9%); ^1H NMR (CDCl_3) δ 6.55 (s, 2 H), 5.85–5.65 (br d, 1 H), 2.95 (br s, 4 H), 1.80–1.20 (d at 1.65, J = 1.5 Hz, 7 H).

In a 100-mL round-bottom flask was dissolved 3.6 g (0.09 mol) of sodium hydroxide in 35 mL of water. The solution was flushed with nitrogen for 30 min, and the system was charged with 3.00 g (0.0148 mol) of **12**. The magnetically stirred solution was cooled to 0 °C and 11.23 g (0.089 mol, 6 equiv) of dimethyl sulfate was added over 30 min with rapid stirring. After 5 h, the solution was no longer alkaline to litmus and a second portion of $\text{NaOH}/(\text{CH}_3)_2\text{SO}_4$ was added in half the original quantities to the solution over 15 min. The solution was stirred overnight, 10 mL of 20% sodium hydroxide was added, and the reaction mixture was stirred at room temperature for an additional 12 h. The aqueous solution was extracted with ether (4 \times 25 mL), and the combined organic layers were dried and concentrated to leave 3.03 g of a brown oil. Chromatography on 125 g of Florisil (hexane-ether, 85:15) gave 2.33 g of a slightly cloudy yellowish oil. A second chromatography on 50 g of Florisil gave 2.23 g of the same oil. Molecular distillation (90 °C oil bath (0.1 mm)) gave 1.92 g (56.3%) of pure **2b** as a clear oil: IR (KBr, cm^{-1}) 3040, 2950, 1495, 1308, 1255, 1095, 1080, 848, 782, 715, 705; ^1H NMR (CDCl_3) δ 6.50 (s, 2 H), 6.00 (d of m, 1 H), 4.30–4.10 (m, 2 H), 3.70 (s, 6 H), 1.80 (d, J = 1.5 Hz, 3 H), 1.45–1.35 (br s, 4 H); m/e calcd 230.1307, obsd 230.1311.

Anal. Calcd for $\text{C}_{15}\text{H}_{18}\text{O}_2$: C, 78.23; H, 7.88. Found: C, 78.38; H, 7.99.

1,4-Dihydro-1,4-ethano-2-iodo-5,6,7,8-tetrafluoronaphthalene (14). A solution of **13** (8.60 g, 0.035 mol) in 20 mL of ethanol containing 0.5 g of 5% palladium on charcoal was hydrogenated in a Parr apparatus at 40 psi for 5 h. The catalyst was separated by filtration, and the filtrate was evaporated to leave 8.62 g (100%) of the dihydro derivative.

A 7.52 g (0.031 mol) sample of this ketone together with 20 mL of hydrazine hydrate and 20 mL of triethylamine was dissolved in 75 mL of ethanol, heated at the reflux temperature for 2 h, poured into 500 mL of hot water, and slowly cooled. The crystals were collected, washed with water, and dried to give 6.0 g (75%) of the hydrazone as colorless crystals, mp 65–66 °C.

Treatment of 6.0 g (0.023 mol) of this hydrazone with triethylamine (80 mL) and iodine (15 g) in 200 mL of tetrahydrofuran as described above afforded 4.06 g (50%) of **14** as colorless crystals: mp 91–92 °C (from hexane); IR (KBr, cm^{-1}) 2980, 2955, 2880, 1595; ^1H NMR (CDCl_3) δ 6.8 (dd, J = 7 and 2 Hz, 1 H), 4.45 (br s, 1 H), 4.25 (br d, 1 H), 2.05–1.2 (m, 4 H); m/e calcd 353.9530, obsd 353.9534.

1,4-Dihydro-1,4-ethano-2-methyl-5,6,7,8-tetrafluoronaphthalene (2c). This olefin was obtained, following the earlier procedure, in 61.5% yield from 4.06 g of **14** after silica gel chromatographic purification. Pure product was obtained as colorless crystals, mp 57.5–58.5 °C (from hexane); ^1H NMR (CDCl_3) δ 5.97 (m, 1 H), 4.3–4.0 (m, 2 H), 1.85 (s, 3 H), 1.65–1.2 (m, 4 H); m/e calcd 242.0718, obsd 242.0722.

Anal. Calcd for $\text{C}_{13}\text{H}_{10}\text{F}_4$: C, 64.46; H, 4.16. Found: C, 64.49; H, 4.28.

1,4-Dihydro-1,4-ethano-2-methyl-5,8-diaminonaphthalene (17a). Benzoquinone adduct **12** (202 mg, 1.0 mmol) was heated at the reflux temperature with 2 mL of a 5% potassium carbonate solution in water-methanol (60:40) for 10 min, poured into water, and extracted with ether. The combined organic phases were washed with water, dried, and evaporated. There was obtained 190 mg (94%) of the hydroquinone, mp 182 °C dec (from benzene-hexane); $^1\text{H NMR}$ (acetone- d_6) δ 7.20 (br s, 2 H), 6.35 (br s, 2 H), 5.92 (d of t, $J = 5$ and 2 Hz, 1 H), 4.30–4.0 (m, 2 H), 1.80 (d, $J = 2$ Hz, 3 H), 1.90–1.10 (m, 4 H); m/e calcd 202.0994, obsd 202.0996.

The hydroquinone (5.70 g, 0.0282 mol) was shaken with 20 g of freshly prepared silver oxide and 20 g of anhydrous sodium sulfate in 150 mL of anhydrous ether for 2 h. The reaction mixture was filtered through Celite, and the filtrate was evaporated to give 5.60 g (98%) of **15** as a yellow solid: mp 59–61 °C; IR (CHCl₃, cm⁻¹) 1645; $^1\text{H NMR}$ (CDCl₃) δ 6.50 (s, 2 H), 5.80 (d of t, $J = 5$ and 2 Hz, 1 H), 4.2–3.9 (br m, 2 H), 1.82 (d, $J = 2$ Hz, 3 H), 1.60–1.15 (br m, 4 H); m/e calcd 200.0837, obsd 200.0841.

A solution of **15** (4.0 g, 0.02 mol) and hydroxylamine hydrochloride (20 g, 0.28 mol) in 300 mL of ethanol was heated at the reflux temperature for 2 h with 5 g of sodium carbonate. The reaction mixture was poured into water (700 mL) and stored in a refrigerator for 2 days. The aqueous phase was extracted with ether and chloroform, and the combined organic extracts were dried and evaporated to leave 5.55 g of residue. This material was chromatographed on silica gel to give 1.75 g of bis(oxime) **16**, 2.55 g of a mixture of monooxime and bis(oxime), and 1.30 mg of pure monooxime. The last two fractions were recycled with hydroxylamine, and an additional 2.51 g of **16** was recovered (total yield 92%). The product melted at 178–180 °C dec; IR (KBr, cm⁻¹) 3440 and 950; $^1\text{H NMR}$ (acetone- d_6) δ 7.20 (s, 2 H), 5.85 (d of t, $J = 5$ and 2 Hz, 1 H), 4.25–4.02 (m, 2 H), 1.82 (d, $J = 2$ Hz, 3 H), 1.60–1.20 (m, 4 H); m/e calcd 230.1055, obsd 230.1059.

A solution of **16** (1.40 g, 6.1 mmol) in a mixture of ethanol (22 mL) and 50% sodium hydroxide solution saturated with ammonium chloride (22 mL) was treated with 2.2 g of ammonium acetate and 5 g of zinc dust and heated at reflux for 3 h. The cooled reaction mixture was filtered, and both the residue and filtrate were extracted with chloroform. The combined organic phases were washed with water, dried, and evaporated to give a residue which was chromatographed on silica gel. There was obtained 1.15 g (97.5%) of **17a** as a brown-purple oil which was difficult to purify: $^1\text{H NMR}$ (CDCl₃) δ 6.10 (s, 2 H), 5.92 (m, 1 H), 3.85–3.50 (m, 5 H), 3.15 (br s, 4 H), 1.5–1.1 (m, 4 H); m/e calcd 200.1313, obsd 200.1318.

1,4-Dihydro-1,4-ethano-2-methyl-5,8-bis(dimethylamino)naphthalene (19). To a cold (0 °C) solution of **17a** (1.5 g, 7.5 mmol) in 10 mL of pyridine was added dropwise with vigorous stirring 1.62 g (15 mmol) of ethyl chloroformate during 15 min. After an additional 15 min, the mixture was poured into ice water (100 mL) and the precipitate was separated by filtration and dried. There was obtained 2.12 g (83%) of **17b**: mp 181–182 °C (from acetone-hexane); $^1\text{H NMR}$ (acetone- d_6) δ 7.90 (m, 2 H), 7.10 (s, 2 H), 5.90 (m, 1 H), 4.25–3.85 (m, 6 H), 1.85 (d, $J = 2$ Hz, 3 H), 1.5–1.0 (m, 10 H); m/e calcd 344.1736, obsd 344.1742.

To 80 mg of sodium hydride (as 50% oil dispersion) in 5 mL of anhydrous tetrahydrofuran was added 500 mg (1.46 mmol) of **17b** dissolved in 12 mL of the same solvent. The resulting mixture was stirred at room temperature until gas evolution ceased. Methyl iodide (365 mL) was introduced via syringe, and the mixture was heated overnight at the reflux temperature. After 6 h, an additional 180 mL of methyl iodide was added. After being cooled, the reaction mixture was filtered, the solvent was evaporated, and the residue was taken up in water. This solution was extracted with ether, and chloroform and the combined organic layers were dried and evaporated. The residual pale brown solid was directly reduced: $^1\text{H NMR}$ (acetone- d_6) δ 6.90 (s, 2 H), 5.90 (m, 1 H), 4.25–3.40 (m, 6 H), 3.15 (s, 6 H), 1.80 (d, $J = 2$ Hz, 3 H), 1.60–0.80 (series of m, 10 H).

This residue was taken up in 5 mL of dry tetrahydrofuran, and this solution was added to a stirred slurry of lithium aluminum hydride (170 mL, 4.5 mmol) in 5 mL of tetrahydrofuran at a rate to maintain gentle reflux. Heating was continued for 5 h. The residue obtained after the usual workup was chromatographed on silica gel (40 g). There was obtained 300 mg (80% from **7b**) of **19** as a colorless oil: $^1\text{H NMR}$ (CDCl₃) δ 6.65 (s, 2 H), 5.95 (m, 1 H), 4.25–4.0 (m, 2 H), 2.65 (s, 12 H), 1.85 (d, $J = 2$ Hz, 3 H), 1.65–1.20 (m, 4 H).

Anal. Calcd for C₁₇H₂₄N₂: C, 79.64; H, 9.44; N, 10.92. Found: C, 79.30; H, 9.58; N, 11.12.

General Photooxygenation Procedure. All photooxygenations were carried out in small reactors with a source of oxygen continuously bubbling through the solution. Rose bengal (1 mg/mL) was used as the sensitizer. The singlet state of oxygen was generated by irradiation of

these solutions with a Sylvania DYV lamp. The allylic hydroperoxides thus formed were reduced in situ with sodium borohydride. The mixture was poured into water, and the aqueous layer was separated and extracted with chloroform. The combined organic layers were washed with 5% sodium hydroxide and water prior to drying. The residue obtained after evaporation of solvent was purified by preparative TLC on basic alumina. For product data see Table IV.

Prototypical Epoxidation Procedure. In a 100-mL round-bottom flask was placed 690 mg (3.0 mmol) of **2b** in 25 mL of chloroform, followed by the dropwise addition of 768 mg (4.45 mmol) of *m*-chloroperbenzoic acid (initially washed with a phosphate buffer solution at pH 7.5 and dried in vacuo) in 25 mL of chloroform at 0 °C. The solution was stirred at this temperature for 3 h and stored at 0 °C overnight. The cloudy solution was washed with 50 mL of water, the water layer was extracted with chloroform (3 × 5 mL), and the combined organic phases were washed with 50 mL each of saturated aqueous Na₂SO₃, NaHCO₃, and NaCl solutions followed by 50 mL of water. After drying and solvent evaporation, the $^1\text{H NMR}$ spectrum of the residue was recorded. The products were isolated by preparative VPC (or TLC). For product data see Table IV.

Simmons-Smith Reaction of 2b. Into a dry 25-mL round-bottom flask fitted with magnetic stirrer and septum was syringed 3.25 mL (3.25 mmol, 5 equiv) of diethylzinc solution⁵⁶ followed by 0.26 mL (870 mg, 3.25 mmol) of CH₂I₂. The mixture was stirred to give a white precipitate which slowly dissolved over 1 h. A solution of 150 mg (0.65 mmol) of **2b** in 5 mL of dry ether was syringed into the stirred solution which was heated at the reflux temperature for 3 h. The solution was cooled and quenched with a few milliliters of 2 N HCl and washed with 10 mL of water, 10 mL of saturated Na₂S₂O₃, and 10 mL of water. The ether phase was dried, filtered, and evaporated to leave 150 mg of a white semi-solid. The $^1\text{H NMR}$ spectrum of this material showed it to be an approximate 1:1 mixture of **2b** and **34b** (lone methyl signal at δ 1.20). Purification was achieved by preparative TLC on silica gel (pentane-ether, 95:5). There was obtained 52.4 mg (33%) of **34b**: mp 121–122 °C; $^1\text{H NMR}$ (CDCl₃) δ 6.60 (s, 2 H), 3.70 (s, 6 H), 3.35 (br s, 1 H), 3.00 (br s, 1 H), 2.0–0.7 (m, 5 H), 1.20 (s, 3 H), –0.10 to –0.40 (t, 1 H), –0.60 to –0.85 (t, 1 H); m/e calcd 244.1463, obsd 244.1468.

Anal. Calcd for C₁₆H₂₀O₂: C, 78.64; H, 8.27. Found: C, 78.50; H, 8.19.

Simmons-Smith Cyclopropanation of 2c. Treatment of 200 mg (0.83 mmol) of **2c** in an analogous manner (4 h) gave a single product in addition to unreacted **2c**. Purification was achieved by preparative VPC (4 ft × 0.25 in. 10% Bentone/10% SF-96 on Chromosorb W, 145 °C): $^1\text{H NMR}$ (CDCl₃) 3.60 (br s, 1 H), 3.30 (br s, 1 H), 1.80–0.90 (m, 5 H), 1.20 (s, 3 H), and –0.70 (br s, 2 H); m/e calcd 256.0875, obsd 256.0881.

syn- and anti-1,2,3,4-Tetrahydro-1,4-ethano-2-methyl-5,8-dimethoxy-2-naphthol (35b and 36b). In a 50-mL round-bottom flask was placed 834 mg (2.62 mmol, 1.2 eq) of mercuric acetate and 10 mL of water. The solution was stirred magnetically until complete dissolution was effected, whereupon a solution of 502 mg (2.18 mmol) of **2b** in 10 mL of tetrahydrofuran was added dropwise within a few minutes to give a bright yellow precipitate. Stirring was continued for 1 h after which time 10 mL of 3 N sodium hydroxide was added with stirring followed by 100 mg (2.62 mmol, 1.2 eq) of sodium borohydride in 10 mL of 3 N NaOH. Stirring was continued for 3 h. The filtered solution was extracted into ether (3 × 15 mL), and the combined ether layers were washed with 15 mL each of saturated sodium bicarbonate solution, water, and brine prior to drying. Solvent concentration furnished 350 mg (64%) of a yellow oil. Purification by preparative TLC on silica gel (elution with ether-pentane, 1:1) gave the following.

Fraction 1: 155.6 mg (29%) of **35b**, mp 59–60 °C; IR (KBr, cm⁻¹) 3500, 3050–2950, 2990, 1601, 1500, 1450, 1325, 1250, 1090, 1000, 950, 915, 790, 755, 710; $^1\text{H NMR}$ (CDCl₃) δ 6.66 (s, 2 H), 3.75 (s, 7 H), 3.60–3.25 (m, 2 H), 2.00–1.25 (m, 9 H); m/e calcd 248.1412, obsd 248.1418. VPC isolation (6 ft × 0.25 in. 5% Carbowax on Chromosorb G, 180 °C) gave the analytical sample.

Anal. Calcd for C₁₅H₂₀O₃: C, 72.55; H, 8.13. Found: C, 72.20; H, 8.08.

Fraction 2: 30 mg (5.5%) of **36b**; IR (KBr, cm⁻¹): 3320, 2950, 2860, 2840, 1600, 1490, 1460, 1370, 1350, 1335, 1315, 1265, 1200, 1130, 1075, 995, 980, 959, 910, 790, 710; $^1\text{H NMR}$ (CDCl₃) δ 6.65 (s, 2 H), 3.75 (s, 7 H), 3.60–3.25 (m, 2 H), 1.75–1.25 (m, 6 H), 1.00 (s, 3 H); m/e calcd 248.1412, obsd 248.1418.

syn- and anti-1,2,3,4-Tetrahydro-1,4-ethano-2-methyl-2-naphthol (35a and 36a). The procedure employed was exactly as described above. From 296 mg (1.74 mmol) of **2a**, 318 mg (3.48 mmol, 2.0 equiv) of mercuric acetate, and 132 mg (2.0 equiv) of NaBH₄, there was obtained 250 mg (76%) of a yellow oil. TLC (silica gel) purification (elution with pentane-ether, 2:1) gave the following.

Table IV. Product Data

starting material (mg)	product(s)	mg isolated (yield, %)	mp, °C	¹ H NMR data (δ, CDCl ₃)	M ⁺ <i>m/e</i> calcd (found)	combustion data
A. Photooxygenation						
2a (230) (acetone)	28a	65 (26)	71–72	7.10 (s, 4 H), 5.0 (m, 2 H), 4.20 (m, 1 H), 3.45 (br s, 1 H), 3.10 (s, 1 H), 1.95–1.10 (m, 5 H)	186.1045 (186.1049)	calcd: C, 83.83; H, 7.58 found: C, 83.81; H, 7.69
	29a	43 (17)	83–84	7.10 (m, 4 H), 5.0 (m, 2 H), 4.02 (m, 1 H), 3.45 (br s, 1 H), 3.10 (m, 1 H), 2.55–1.05 (m, 5 H)		calcd: C, 83.83; H, 7.58 found: C, 83.51; H, 7.54
2b (402) (methanol)	29b	27 (6.3)		6.52 (s, 2 H), 5.0 (m, 2 H), 3.5–3.4 (m, 9 H), 2.3–1.0 (m, 5 H)	246.1256 (246.1260)	
	28b	31 (7.2)		6.52 (s, 2 H), 5.0 (m, 2 H), 4.3–3.5 (m, 9 H), 1.80–1.10 (m, 5 H)	246.1256 (246.1260)	
2c (242) (acetone)	28c/29c (inseparable)	55 (21)		4.30 for 28c and 4.10 for 20c		calcd: C, 60.51; H, 3.91 found: C, 60.20; H, 4.03
B. Epoxidation						
2b (690)	33b	35 (5)	oil	6.65 (s, 2 H), 3.75 (s, 6 H), 3.77–3.55 (m, 2 H), 3.1 (d, <i>J</i> = 4 Hz, 1 H), 2.0–1.9 and 1.1–0.9 (2d, <i>J</i> = 6 Hz, 4 H), 1.25 (s, 3 H)	246.1256 (246.1260)	
	32b	330 (47)	137.5–138.5	6.65 (s, 2 H), 3.70 (s, 6 H), 3.8–3.6 (m, 2 H), 3.1 (d, <i>J</i> = 4 Hz, 1 H), 1.8–1.2 (m, 4 H), 1.5 (s, 3 H)	246.1256 (246.1260)	calcd: C, 73.14; H, 7.38 found: C, 72.96; H, 7.32
2a (149)	32a	57 (35)	oil	7.1 (s, 4 H), 3.2–3.1 (m, 2 H), 3.1 (d, <i>J</i> = 4 Hz, 1 H), 2.0 (m, 2 H), 1.2 (s, 3 H), 1.1 (m, 2 H)	186.1045 (186.1048)	
	33a	36.8 (22)	oil	7.1 (s, 4 H), 3.2–3.1 (m, 2 H), 3.1 (d, <i>J</i> = 4 Hz, 1 H), 2.0 (m, 2 H), 1.2 (s, 3 H), 1.1 (m, 2 H)	186.1045 (186.1048)	
2c (159)	32c	58.1 (34)	oil	3.8 (br s, 1 H), 3.5 (br s, 1 H), 3.05 (d, <i>J</i> = 4 Hz, 1 H), 1.90–1.25 (m, 4 H), 1.50 (s, 3 H)	258.0668 (258.0671)	calcd: C, 60.46; H, 3.91 found: C, 60.32; H, 3.95
	33c	15.9 (9.3)	oil	3.75 (br s, 1 H), 3.5 (br s, 1 H), 3.1 (d, <i>J</i> = 4 Hz, 1 H), 2.1–1.0 (m, 4 H), 1.25 (s, 3 H)	258.0668 (258.0671)	
C. Hydroboration						
2b (141)	37b	92 (61)	72.5–73.5	6.55 (s, 2 H), 3.65 (s, 6 H), 3.45 (br s, 2 H), 3.20 (br s, 1 H), 1.8–1.2 (br m, 9 H)	248.1412 (248.1420)	calcd: C, 72.54; H, 8.13 found: C, 72.29; H, 7.99
	38b	36 (24)	91–93	6.60 (s, 2 H), 3.75 (s, 6 H), 3.4 (br s, 1 H), 3.2 (m, 2 H), 2.2–1.2 (m, 7 H), 0.8 (d, <i>J</i> = 8 Hz, 3 H)	248.1412 (248.1420)	
2a	38a	(33.3)	88–91	7.1 (s, 4 H), 3.25 (s, 1 H), 2.95 (s, 1 H), 2.60 (s, 1 H), 1.8–1.2 (m, 6 H), 0.8–0.7 (d, <i>J</i> = 8 Hz, 3 H)	188.1201 (188.1206)	
	37a	(66.7)	62–63.5	7.15 (s, 4 H), 3.40 (s, 1 H), 3.0 (s, 1 H), 2.7 (s, 1 H), 1.8–1.2 (m, 6 H), 1.2 (s, 3 H)	188.1201 (188.1206)	calcd: C, 82.92; H, 8.58 found: C, 82.66; H, 8.47
2c	38c	(6)		3.20 (br, s, 2 H), 2.6 (br s, 1 H), 2.1–1.2 (m, 6 H), 0.8–0.7 (d, <i>J</i> = 7 Hz, 3 H)	260.0824 (260.0833)	
	37c	(94)		3.60 (br s, 1 H), 3.40 (br s, 1 H), 3.20 (s, 1 H), 1.80–1.20 (m, 6 H), 1.20 (s, 3 H)	260.0824 (260.0833)	calcd: C, 59.99; H, 4.66 found: C, 60.10; H, 4.62

Fraction 1: 33.1 mg (6.6%) of **36a**; IR (KBr, cm⁻¹) 3325, 2930, 3865, 1480, 1455, 1370, 1210, 1120, 1090, 910, 750; ¹H NMR (CDCl₃) δ 7.10 (s, 4 H), 3.0 (br s, 1 H), 2.7 (br s, 1 H), 1.90–1.25 (m, 7 H), 6.90 (s, 3 H); *m/e* calcd 188.1201, obsd 188.1207.

Fraction 2: 120 mg (37%) of **35a**, mp 81.5–82.5 °C; IR (KBr, cm⁻¹) 3320, 2930, 2870, 1485, 1370, 1328, 1265, 1235, 1181, 1160, 1120, 1039, 910, 750, 700; ¹H NMR (CDCl₃) δ 7.1 (s, 4 H), 3.0 (br s, 1 H), 2.8 (br s, 1 H), 2.0–1.2 (m, 7 H), 1.4 (s, 3 H); *m/e* calcd 188.1201, obsd 188.1207.

Anal. Calcd for C₁₃H₁₆O: C, 82.96; H, 8.58. Found: C, 82.81; H, 8.53.

General Hydroboration Procedure. Into a dry 15-mL round-bottom flask fitted with a magnetic stirrer was placed a solution of 141 mg (0.61 mmol) of **2b** in 10 mL of tetrahydrofuran. The solution was stirred while cooled to 0 °C, whereupon 16.9 mg (0.61 mmol, 0.64 mL of a 0.95 M solution in tetrahydrofuran) of diborane was slowly introduced via syringe. Stirring was continued at room temperature for an additional 30 min. The progress of reaction was arrested by the careful addition of 2 mL of water, and oxidation was carried out by the addition of 0.2 mL of 3 N sodium hydroxide (0.6 mmol) followed by 0.17 mL of 30% hy-

drogen peroxide (1.5 mmol). The solution was stirred at 30–50 °C for 1 h, shaken with 400 mg of potassium carbonate in 10 mL of water, and partially evaporated to leave an aqueous residue. The products were extracted with ether (3 × 15 mL), dried, filtered, and concentrated to a clear oil or semi-solid (130–140 mg, 90–100%). For product data see Table IV.

Reduction of 32. Into a 15-mL round-bottom flask fitted with a magnetic stirrer and flushed with nitrogen gas was placed 35 mg (0.14 mmol) of **32** dissolved in 5 mL of dry tetrahydrofuran followed by 90.0 mg (0.85 mmol, 90 μL of a 1 M solution in tetrahydrofuran) of LiEt₃BH via syringe. The solution was stirred while being heated for 25 h, hydrolyzed with 1 mL of water, and the intermediate organoborane oxidized with 0.20 mL of 30% hydrogen peroxide and 0.28 mL of 3 N sodium hydroxide. The mixture was partially evaporated to leave an aqueous residue from which the product was extracted with ether (4 × 5 mL). The combined ether phases were washed with 20 mL of saturated sodium bicarbonate solution and 20 mL of brine, dried, filtered, and concentrated to leave 40 mg of white solid. Preparative TLC purification on silica gel (elution with pentane–ethyl acetate, 85:15) gave 20 mg (57%) of **35b**. Trituration and then crystallization from pentane gave white crystals, mp

59–60 °C, the spectral properties of which were identical to those of the original sample.

Competitive Rate Studies. Since the relative rates of each reaction were measured by VPC analysis of the ratio of unreacted starting materials, the detector responses to **2a–c** were calibrated. This was accomplished by the preparation of standard solutions of the olefins containing an internal standard and VPC analysis of the mixtures to obtain correction factors according to eq 2.⁵⁷

$$F = \left[\frac{(\text{wt of olefin})(\% \text{ purity})}{(\text{wt of standard})(\% \text{ purity})} \right] \left[\frac{\text{standard area}}{\text{olefin area}} \right] \quad (2)$$

Since it was necessary (because of retention times) to use two sets of VPC parameters, one for comparing olefins **2a** and **2b** and another for

(57) (a) Rawson, R. J. *J. Org. Chem.* **1970**, *35*, 2027. (b) Sawoda, S. *Bull. Chem. Soc. Jpn.* **1969**, *42*, 2669.

(58) Casazza, W. T.; Staltenkamp, R. J. *J. Gas Chromatog.* **1965**, *253*.

2a and **2c**, two standard solutions were prepared by using two separate internal standards (dibenzyl ether and 2-methylnaphthalene, respectively).

Three VPC traces were made for each solution and the average of the relative areas measured by an accurate weighing of the photoreproduced peaks of the chromatographs.

The reactions were conducted as described earlier using a limiting amount of electrophile (0.4 equiv) on a mixture of **2a** and **2b** or **2a** and **2c**, followed by analysis of unreacted starting materials. The reaction conditions were precisely those used to ascertain stereoselectivities of each substrate–reagent pair. Each reaction was run in duplicate to assure reproducibility.

Acknowledgment. This investigation was supported by grants from the National Cancer Institute (Grant CA-12115), the Deutsche Forschungsgemeinschaft, the Fonds der Chemischen Industrie, and BASF Ludwigshafen.

Gas-Phase Reactions of Negative Ions with Alkyl Nitrites

Gary K. King, M. Matti Maricq, Veronica M. Bierbaum, and Charles H. DePuy*

Contribution from the Department of Chemistry,
University of Colorado, Boulder, Colorado 80309. Received April 29, 1981

Abstract: The gas-phase reactions of F^- , NH_2^- , OH^- , and a variety of carbanions with a series of alkyl nitrites (methyl, ethyl, *n*-butyl, isoamyl, and neopentyl) are reported. The reactions of F^- were studied by the selected ion flow tube technique while all other reactions were examined in a conventional flowing afterglow system. For fluoride ion, E2 reactions occur exclusively for nitrites containing β -hydrogens, S_N2 processes dominate for methyl nitrite, and E_{CO2} reactions occur for neopentyl nitrite. The high specificity of product formation is discussed in terms of potential surfaces, and reaction rate constants are compared to calculated collision rates. The reactions of carbanions with neopentyl nitrite proceed primarily by nitrosation followed by proton transfer or by nitrosation followed by a reverse Claisen-type condensation. Finally, NH_2^- and OH^- react rapidly with most nitrites to form NO_2^- ; NH_2^- reacts with neopentyl nitrite to generate HN_2O^- . These data are compared and contrasted to some recent results from ion cyclotron resonance experiments.

Introduction

Alkyl nitrites are highly reactive reagents¹ capable of undergoing many different types of reactions, both in solution and in the gas phase. The nitroso group is electrophilic and hence susceptible to attack by nucleophiles; in solution carbanions react readily with alkyl nitrites, forming nitroso compounds and, by tautomerization, oximes. The mechanism involves a typical Claisen-type condensation which has often been exploited in synthesis. The nitrite ion is also a potentially good leaving group in substitution and elimination reactions. Thermally and photochemically, alkyl nitrites undergo homolytic cleavage to form NO and alkoxy radicals. This great diversity of reaction pathways makes nitrites potentially useful substrates for gas-phase ion synthesis reactions and for studies of the mechanisms of gas-phase ion–molecule interactions.

Although alkyl nitrites have been widely used as sources of alkoxide ions upon their interaction with low-energy electrons, relatively little is known about their gas-phase ion–molecule chemistry. McAllister and Pitman² have compared the ion–molecule reactions of methyl nitrite and nitromethane in an ion cyclotron resonance (ICR) experiment. McMahon and Farid³ have studied some of the primary and secondary products resulting

from electron impact on a series of alkyl nitrites. Recently, Noest and Nibbering⁴ have described negative ion reactions of a variety of alkyl nitrites in an ICR, and Klass and Bowie⁵ have reported the reactions of a series of enolate ions with methyl nitrite also in an ICR spectrometer.

In this paper we report a flowing afterglow (FA) and selected ion flow tube (SIFT) study of the reactions of methyl, ethyl, *n*-butyl, isoamyl, and neopentyl nitrites with a variety of negative ions. The reactions of fluoride ion proceed by substitution and/or elimination channels and shed some new light on the mechanisms and energy surfaces of gas-phase ion–molecule reactions. Carbanions react in the gas phase mainly as they do in solution, i.e., by nitrosation. The resulting nitroso compounds, however, can undergo further interesting and informative fragmentation reactions which imply the existence of long-lived ion–dipole complexes.

Our results reveal some important and intriguing differences between gas-phase ion–molecule chemistry in the relatively high-pressure (0.5 torr) regime of the FA and in the low-pressure (10^{-5} torr) technique of ICR spectroscopy.

Experimental Section

The reactions of alkyl nitrites with amide ion, hydroxide ion, and a variety of carbanions were carried out in a conventional flowing afterglow apparatus which has been described previously.⁶ Typical pressures and

(1) March, J. "Advanced Organic Chemistry", 2nd ed.; McGraw-Hill: New York, 1977.

(2) McAllister, T.; Pitman, P. *Int. J. Mass Spectrom. Ion Phys.* **1976**, *19*, 241–248.

(3) McMahon, T. B.; Farid, R. *Int. J. Mass Spectrom. Ion Phys.* **1978**, *27*, 163–183.

(4) Noest, A. J.; Nibbering, N. M. M. *Adv. Mass Spectrom.* **1980**, *8*, 227–237.

(5) Klass, G.; Bowie, J. H. *Aust. J. Chem.* **1980**, *33*, 2271–2275.

(6) DePuy, C. H.; Bierbaum, V. M. *Acc. Chem. Res.* **1981**, *14*, 146–153.